Two sites of Fe^{3+} in highly Mg-doped $LiNBO_3$

LETTER TO THE EDITOR

Two sites of Fe^{3+} in highly Mg-doped $LiNbO_3$

A Böker†, H Donnerberg†, O F Schirmer† and Feng Xiqi‡

† Fachbereich Physik, Universität Osnabrück, D-4500 Osnabrück, Federal Republic of Germany
‡ Academia Sinica, Shanghai Institute of Ceramics, Shanghai, People's Republic of China

Abstract. Two species of Fe^{3+} ESR have been observed in $LiNbO_3$:6%Mg codoped with 530 ppm Fe. Their axial crystal field parameters, D, differ by a factor of about two. As indicated by a superposition model analysis, it is likely that the centre with the large D has to be attributed to Fe_{Li}^{3+}, and that with the low D to Fe_{Nb}^{3+}. This assignment is also supported by recent shell model calculations of the incorporation mechanism of impurities in $LiNbO_3$.

Doping $LiNbO_3$ with a high concentration of Mg, $[Mg] \geq 5\%$, increases its photo-conductivity, σ_{ph} [1], and thus reduces its optical damage [2]. In an analogous way the dark conductivity of reduced crystals rises strongly with Mg doping. This is due to the fact that deep traps, most likely Nb_{Li}, which lead to an activation energy for conductivity of about 0.65 eV in reduced material [3], are removed by Mg doping. Such crystals have an activation energy of only ≈ 0.16 eV [4]. These results refer to crystals nominally free of Fe.

In Fe-doped crystals the lattice position of Fe^{3+}, and therefore probably also its electrical properties, are changed by sufficiently high Mg doping. This is known from ESR studies first reported by Halliburton and co-workers [5]. At microwave frequencies of 9 GHz a pronounced change of the Fe^{3+} signals was observed, if $[Mg]$ rises above 5%. It has been proposed that the new Fe^{3+} spectra are due to Fe^{3+} on a Nb site. Similar observations were recently published by Feng and Tang [6]. No analysis of the new Fe^{3+} spectra has been given in these papers. Here we present ESR measurements performed at 34 GHz with $LiNbO_3$ grown from a congruent melt containing 6 mol% MgO and 530 ppm Fe. Two types of Fe^{3+} spectra were identified. We report the ESR parameters describing the spectra and analyse them in terms of the superposition model [7]. Also the incorporation of Fe into $LiNbO_3$ doped with Mg will be discussed on the basis of the energetics of relevant chemical reactions as derived from recent shell model simulations of defective $LiNbO_3$.

Figure 1 shows the ESR spectrum of the above crystal. Two superimposed spectra are seen, each being described by the Hamiltonian [8]

$$\mathcal{H} = \beta(\boldsymbol{B} \cdot \boldsymbol{g} \cdot \boldsymbol{S}) + \tfrac{1}{6}a[\hat{S}_x^4 + \hat{S}_y^4 + \hat{S}_z^4 - \tfrac{1}{5}S(S+1)(3S^2+3S-1)] + D[\hat{S}_{z'}^2 - \tfrac{1}{3}S(S+1)]$$
$$+ \tfrac{1}{180}F[35\hat{S}_{z'}^4 - 30S(S+1)\hat{S}_{z'}^2 + 25\hat{S}_{z'}^2 - 6S(S+1) + 3S^2(S+1)^2].$$
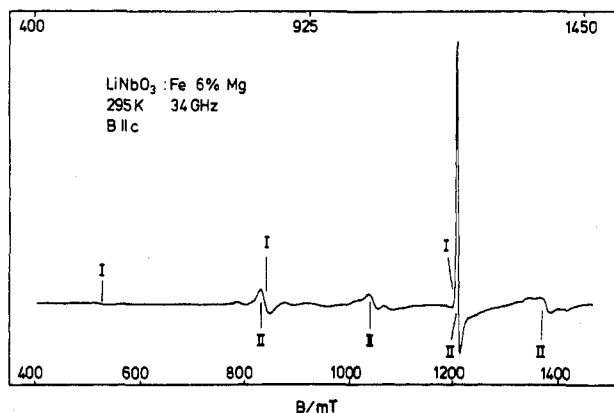
Figure 1. ESR of $LiNbO_3$ (congruently melting composition, 6 mol% MgO and 530 ppm Fe in the melt). The assignment to centres I and II is indicated. At high fields the spectra are truncated because of magnet limitations. The origin of the satellite line pair near the $\frac{3}{2} \leftrightarrow \frac{1}{2}$ transitions is not yet known.

The spectra have been found to be axially symmetric. For the orientation $B\|c$ there exists an exact solution of the above Hamiltonian [9], yielding the following parameters:

|	Spectrum I	Spectrum II
$g_\|$	2.001 ± 0.003	2.000 ± 0.002
D	1760 ± 8 G	896 ± 3 G
$a - F$	110 ± 8 G	-93 ± 6 G

The parameters in set I are in agreement with those reported for Fe^{3+} in $LiNbO_3$ not containing Mg [10]; this corresponds to the lines indicated as I in figure 1. The changed environment of Fe^{3+} in highly Mg-doped material is represented by set II: most conspicuous is the fact that D_{II} is only half of D_I. This corresponds to the much smaller splittings of spectrum II as compared to I in figure 1.

Using the Newman superposition model [7], information with respect to the position of the Fe^{3+} within its O^{2-} environment can be extracted from the D-values. Agulló-López and Müller [11] have discussed the position of Fe^{3+} on this basis. The parameter D is given in this method by

$$D = b_2^0 = \tfrac{1}{2}\overline{b_2}(R_0) \left(\sum_{i=1}^{6} \left(\frac{R_0}{R_i} \right)^{t_2} (3\cos^2 \Theta_i - 1) \right) \tag{1}$$

where $\overline{b_2}$, t_2 are experimentally determined parameters for Fe^{3+} in a sixfold-coordinated O^{2-} environment. They were taken as $\overline{b_2}(R_0) = -0.41\,\text{cm}^{-1}$ and $t_2 = 8$ [12], respectively. R_i and Θ_i are polar coordinates of the ith O^{2-} ion neighbouring Fe^{3+} with respect to the c axis of the crystal. These latter parameters were obtained from crystallographic data [13]. R_0 is the reference distance chosen near the value of the R_i ($R_0 = 2.101$ Å). The two curves in figure 2 show the calculated dependence of the b_2^0 parameters on the z coordinates, as defined in figure 3 for both Li and Nb sites in $LiNbO_3$ neglecting possible small corrections for charge misfits. These results are based on the assumption that the relaxation of O^{2-} ligands is small compared to that of the Fe^{3+} ions. The two horizontal
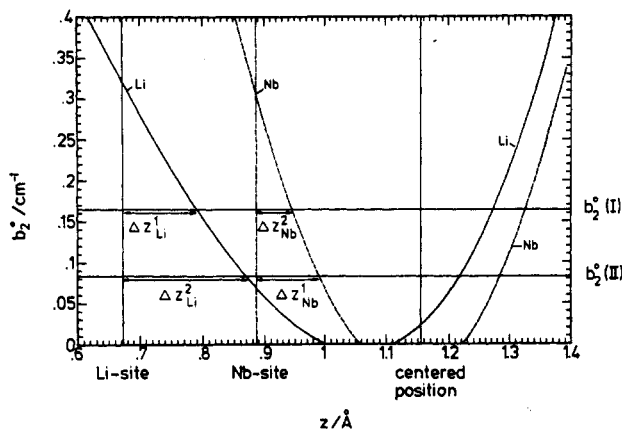
Figure 2. Superposition model predictions of parameters b_2^0: Fe_{Nb}^{3+} ($-\ -\ -$), Fe_{Li}^{3+} (————), as compared with the experimental data.
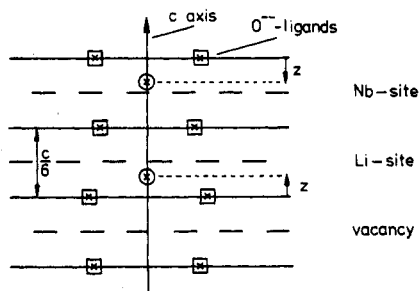
Figure 3. Geometry of $LiNbO_3$ as used in the superposition model calculations. The variation of the parameter z, as defined in the present figure, leads to the curves in figure 2.

lines mark the experimental values of b_2^0. Their crossings with the curves occur at the z values predicted by the model. It is natural to assume that Fe^{3+} will be found closest to the nominal positions of either Li^+ or Nb^{5+}. We thus discard the z values near 1.25 Å as possible explanations of the experimental b_2^0 values. Also recent shell model calculations [14] show that replacement occurs close to the nominal positions.

Agreement between theory and experiment is found when $Fe^{3+}(I)$ is assumed to be close to the Li site (displaced towards centred position by $\Delta z_{Li}^1 \simeq 0.1$ Å) and $Fe^{3+}(II)$ close to the Nb site ($\Delta z_{Nb}^1 \simeq 0.1$ Å).

This assignment is in accord with the fact that Fe^{3+} is found by ENDOR investigations at a Li site in the isostructural $LiTaO_3$ [15]. Also recent EXAFS studies of $LiNbO_3$:Fe indicate that Fe (in the absence of Mg) replaces Li [16]. The present assignment is furthermore supported by the results of a shell model calculation [14] that the energetically most favourable incorporation of both Mg^{2+} and Fe^{3+} in congruent material occurs by replacing Nb_{Li}^{5+} antisite defects. Under the assumption that all Nb_{Li} antisite defects are replaced by Mg ions the presence of Fe^{3+} on both sites is energetically favourable according to self-compensation.

While these arguments show that the assignment of I to Fe_{Li}^{3+} and II to Fe_{Nb}^{3+} is reasonable for both geometrical and energetic reasons, other possibilities should also

be discussed. The converse assignment, Fe_{Nb}^{3+} to I and Fe_{Li}^{3+} to II, would be reconcilable with the information in figure 2 only when Fe^{3+} is displaced from the Li site by the comparatively large $\Delta z_{Li}^2 \simeq 0.2$ Å. This is less likely than the shorter displacements following from the previous assignment. One has also to consider the possibility that one of the Fe^{3+} species is accommodated at the structural vacancy of $LiNbO_3$. Shell model calculations [14] again show that cations at this position are unfavourable energetically.

It is furthermore conceivable that $Fe^{3+}(II)$ is due to an association of the rather abundant Mg on a neighbouring cation site, most likely Mg_{Li}. Because of the axiality of the ESR spectra, $Mg_{Li}-Fe_{Nb}$ pairs not oriented along the c axis are to be ruled out. Such a preferential pair orientation appears to be rather unlikely. Summarising, we favour $Fe^{3+}(II)$ as being Fe_{Nb}^{3+}.

References

[1] Bryan D A, Rice R R, Gerson R, Tomaschke H E, Sweeney K L and Halliburton L E 1985 *Opt. Eng.* **24** 138

[2] Zhong G G, Jian J and Zhong-Khang W 1980 *IEEE Cat.* **80** CH 1561-0, p 631

[3] Nagels P 1980 *The Hall Effect and its Application* ed C L Chien and C R Westlake (New York: Plenum) p 253

[4] Koppitz J, Kuznetsov A I, Schirmer O F, Wöhlecke M, Wörner R and Grabmaier B C 1988 *Proc. SPIE* **1018** 23

[5] Sweeney K L, Halliburton L E, Bryan D A, Rice R R, Gerson R and Tomaschke H E 1985 *J. Appl. Phys.* **57** 1036

[6] Feng Xiqi and Tang Lianan 1990 *Ferroelectrics* at press

[7] Newman D J 1971 *Adv. Phys.* **20** 197
    Newman D J and Urban W 1975 *Adv. Phys.* **24** 793

[8] Abragam A and Bleaney B 1970 *Electron Paramagnetic Resonance of Transition Ions* (Oxford: Clarendon)

[9] Schneider J 1962 *Z. Naturf.* a **17** 189

[10] Herrington J B, Dischler B and Schneider J 1972 *Solid State Commun.* **10** 509

[11] Agulló-López F, Müller K A 1987 *Cryst. Latt. Defects Amorph. Mater.* **15** 89

[12] Siegel E and Müller K A 1979 *Phys. Rev.* B **19** 109

[13] Abrahams S C and Marsh P 1986 *Acta. Crystallogr.* B **42** 61

[14] Donnerberg H, Tomlinson S M, Catlow C R A and Schirmer O F 1989 *Phys. Rev.* B **40** 11909; and to be published

[15] Söthe H, Rowan L G and Spaeth J M 1989 *J. Phys.: Condens. Matter* **1** 3591

[16] Catlow C R A private communication